

Quantum stochastic resonance in the strong-field limit

Ke Dong¹ and Nancy Makri^{1,2}¹*Departments of Physics, University of Illinois, 1110 West Green Street, Urbana, Illinois 61801, USA*²*Department of Chemistry, University of Illinois, 601 South Goodwin Avenue, Urbana, Illinois 61801, USA*

(Received 1 July 2003; revised manuscript received 30 June 2004; published 5 October 2004)

Numerical path integral calculations are performed to study the behavior of a dissipative two-level system driven by a strong monochromatic oscillatory field. It is shown that the population of an initially localized state displays persistent high-frequency oscillations at weak dissipation and low temperature. The oscillation amplitudes exhibit intricate patterns as the field parameters are varied. The observed behavior is an extension of the quantum stochastic resonance phenomenon outside the weak-field regime.

DOI: 10.1103/PhysRevA.70.042101

PACS number(s): 03.65.Yz, 02.50.Ey, 05.10.Gg

I. INTRODUCTION

It is well-known that a symmetric two-level system (TLS) combined with a fast monochromatic external field is equivalent (to zeroth order) to another TLS with a renormalized tunneling splitting [1]. Coupling a TLS to a dissipative bath results in rich dynamical behaviors characterized by a crossover from damped oscillations to exponential decay [2]. Not surprisingly, a TLS interacting with a high-frequency external driving field and a dissipative bath is equivalent (to zeroth order) to another TLS with a renormalized tunneling splitting coupled to the same dissipative bath. In fact, driven dissipative TLS's in the weak dissipation regime exhibit crossover behavior from a damped oscillation regime to one where the decay is exponential [3]; both of these regimes have been observed in numerical calculations [4–6]. In addition, the interplay among a system's intrinsic dynamics, dissipation and external driving also results in some novel physical phenomena, such as a nonlinear dependence of oscillation amplitude on dissipation known as stochastic resonance [7].

Dissipation is generally associated with the destruction of coherence. As an exception to that conventional wisdom, stochastic resonance (SR) in bistable systems is an intriguing phenomenon where the response of driven systems with persistent coherences is enhanced due to the cooperative interaction among random noise, bistability, and periodic forcing. At zero temperature only quantum stochastic resonance (QSR) survives, and the nonlinear response of a driven quantum mechanical system originates in quantum noise. QSR in symmetric TLS's has been studied in the limit of small dissipation and weak fields [8]. At resonant driving, QSR manifests itself as a nonmonotonic response with driving field strength, and optimal response is achieved at a field amplitude proportional to the TLS relaxation rate. Thus, earlier work in the weak field regime predicted a single maximum of the TLS steady-state oscillation amplitude. The latter is a function of temperature and independent of bath properties. In this regime increase of the external field strength above the optimal value leads to a monotonic decrease of the TLS oscillation amplitude. Asymmetric TLS's have been studied in the high-frequency regime, where resonance was observed when the driving frequency approaches fractional values of the static detuning energy [9,10].

The present article extends these previous studies to strong fields. For much of the parameter space of interest the renormalized dissipative TLS Hamiltonian lies outside of the regime that can be reliably treated by analytic approximations, so we resort to a numerical treatment of the driven dissipative TLS. Quantum mechanical simulation of the dynamics of driven systems coupled to dissipative environments has become possible in the last decade through the development of an iterative procedure for evaluating the path integral expression for the reduced density matrix of the system [11–17], where the effects of the dissipative bath enter via an influence functional [18]. This numerically exact methodology has enabled many studies of dissipative TLS's in regimes not accessible to approximate treatments [5,6,8,19,20] and is employed in the present studies of QSR under strong driving. The results of our calculations reveal a complex dependence of the QSR amplitude on the parameters of the applied field and the strength of dissipation. Specifically, we observe secondary and tertiary peaks, as well as local minima and near-localization points, that are absent in the weak-field regime.

Section II introduces the model Hamiltonian and reviews the numerical path integral methodology employed in the calculations. Typical behaviors of the driven dissipative TLS are presented in Sec. III, and the results are summarized by displaying the complex dependence of the long-time TLS oscillation amplitude on dissipation strength and field amplitude. In Sec. IV we present a semiquantitative interpretation of the numerical results by resorting to the quantized representation of the radiation field. Finally, Sec. V presents some concluding remarks.

II. MODEL AND NUMERICAL METHODOLOGY

The system under consideration is described by the following dissipative TLS Hamiltonian driven by a monochromatic field

$$\hat{H}_{\text{SFB}} = -\frac{1}{2}\hbar\Delta\hat{\sigma}_x + \hat{\sigma}_z V_0 \cos \omega t + \sum_j \left[\frac{p_j^2}{2m_j} + \frac{1}{2}m_j\omega_j^2 x_j^2 + c_{jx}x_j\hat{\sigma}_z \right]. \quad (1)$$

Here $\hbar\Delta$ is the splitting of the free tunneling doublet, V_0 and

ω describe the field strength and frequency, l is a length parameter, and we have used the operators $\hat{\sigma}_x = |L\rangle\langle R| + |R\rangle\langle L|$ and $\hat{\sigma}_z = |R\rangle\langle R| - |L\rangle\langle L|$, where the localized state $|L\rangle$ and $|R\rangle$ represent the “left” and “right” TLS sites. The time-dependent term in Eq. (1) represents the electromagnetic radiation field in its semiclassical description. The bath’s dissipative effects on the dynamics of the system can be described by the spectral function

$$J(\omega) = \frac{\pi}{2} \sum_j \frac{c_j^2}{m_j \omega_j} \delta(\omega - \omega_j), \quad (2)$$

which is practically a continuous function for macroscopic environments. The “Ohmic bath” described by the spectral function $J(\omega) = \eta \omega \exp(-\omega/\omega_c)$, where η is the friction coefficient and ω_c is the cutoff frequency of the bath, is a convenient and widely used model of dissipative environments. The strength of the friction can be described by the dimensionless Kondo parameter $\alpha = 2\eta l^2 / \pi \hbar$.

The time-dependent properties of the driven dissipative TLS can be obtained from the reduced density operator

$$\tilde{\rho}(t) = \text{Tr}_B[\hat{U}(t,0)\hat{\rho}(0)\hat{U}^{-1}(t,0)], \quad (3)$$

where $\hat{U}(t'',t')$ is the evolution operator for the time-dependent Hamiltonian of Eq. (1) and Tr_B denotes the trace with respect to the harmonic bath. The path integral representation of the reduced density matrix in Eq. (3) takes the form [14]

$$\begin{aligned} \langle \sigma'' | \tilde{\rho}(t) | \sigma' \rangle &= \sum_{\sigma_0^{\pm}=\pm 1} \sum_{\sigma_1^{\pm}=\pm 1} \cdots \sum_{\sigma_{N-1}^{\pm}=\pm 1} \sum_{\sigma_0^{\mp}=\pm 1} \sum_{\sigma_1^{\mp}=\pm 1} \cdots \sum_{\sigma_{N-1}^{\mp}=\pm 1} \\ &\times \langle \sigma'' | \hat{U}_0(t, t - \delta t) | \sigma_{N-1}^+ \rangle \cdots \langle \sigma_1^+ | \hat{U}_0(\delta t, 0) | \sigma_0^+ \rangle \\ &\times \langle \sigma_0^+ | \tilde{\rho}(0) | \sigma_0^- \rangle \langle \sigma_0^- | \hat{U}_0^{-1}(\delta t, 0) \\ &\times | \sigma_1^- \rangle \cdots \langle \sigma_{N-1}^- | \hat{U}_0^{-1}(t, t - \delta t) | \sigma' \rangle \\ &\times F(\sigma_0^+, \sigma_1^+, \cdots, \sigma_{N-1}^+, \sigma'', \sigma_0^-, \sigma_1^-, \cdots, \sigma_{N-1}^-, \sigma'; \delta t), \end{aligned} \quad (4)$$

where δt is a sufficiently small time step, $\sigma = L$ or R is a discrete variable indicating the TLS state, $\hat{U}_0(t', t'')$ is the time evolution operator for the dissipationless driven TLS, and

$$F = \exp\left(-\frac{1}{\hbar} \sum_{k=0}^N \sum_{k'=0}^k (\sigma_k^+ - \sigma_k^-) (\eta_{kk'} \sigma_{k'}^+ - \eta_{kk'}^* \sigma_{k'}^-)\right) \quad (5)$$

is a discretized version of the Feynman-Vernon influence functional [18] where the coefficients $\eta_{kk'}$ constitute the discrete analog of the bath response function [21]. The superscripts \pm in Eq. (4) refer to forward and backward paths that evolve in the positive and negative time directions [22]. The discretized path integral representation of the TLS reduced density matrix contains nonlocal terms through the double sum in Eq. (5). Nevertheless, the bath response function characterizing dissipative environments drops off rapidly with time. This feature is a consequence of dephasing in media with broad spectra and implies that “long memory”

terms make negligible contribution to the dynamics. As a result, the magnitude of the coefficients $\eta_{kk'}$ decreases rapidly as a function of $|k-k'|$ [11]. Retaining terms with $|k-k'| \leq \delta k_{\max}$, where $\delta k_{\max} \delta t$ is the effective memory length, leads to a quasi-Markovian dynamics and allows evaluation of Eq. (4) via an iterative scheme.

The calculations presented in the next section were performed with bath cutoff frequency $\omega_c = 8.256\Delta$ at a temperature $\beta = 1/k_B T = 5.813 \hbar^{-1} \Delta^{-1}$. In most cases presented in this paper converged results were obtained with the path integral time step $\delta t = 0.08(2\pi/\Delta)$ and truncation of nonlocal influence functional interactions at $\delta k_{\max} = 6$.

III. SIMULATION RESULTS

Figure 1 shows the average position of the driven TLS for $\omega = 5\Delta$. Results for select values of the field amplitude are presented for the bare driven TLS and for the same system in the presence of dissipation. The dynamics is characterized by complex patterns, and diverse behaviors are seen to arise with different field amplitudes. Exact localization in the absence of dissipation is attained when the ratio $2V_0/\hbar\omega$ corresponds approximately (but not exactly) to a zero of the zeroth-order Bessel function. In some of the cases displayed in Fig. 1 the average position of the driven dissipative TLS is seen to exhibit persistent high-frequency oscillations at long time. These are analogous to the QSR oscillations observed earlier for resonant driving at small values of the driving field [8].

The long-time steady-state amplitude exhibits a nonmonotonic dependence on field amplitude. The dependence of this steady-state amplitude on the field strength is shown in Fig. 2. It is seen that varying the external field parameters can lead to very complicated patterns in the long-time oscillation amplitude. At resonant driving the first peak corresponds to the QSR identified earlier in the weak field and small dissipation limit [8]. Similar (though not identical) patterns are observed here with higher driving frequencies and stronger fields. For $\omega > \Delta$, the long-time TLS amplitude nearly vanishes near field amplitudes for which $J_0(2V_0/\hbar\omega) = 0$ and exhibits local minima in the vicinity of parameters that satisfy $J_1(2V_0/\hbar\omega) = 0$. Deep and secondary minima are also observed in the case of resonant driving ($\omega = \Delta$), but the first minimum is not as deep in this case and its location is shifted considerably.

We also study in detail the long-time amplitude of coherent oscillation at resonant driving as a function of the Kondo parameter α and the external field parameter $2V_0/\hbar\omega$ in the region between the first and the second resonant peak. As shown in Fig. 3, the amplitude of coherent oscillation exhibits a peak as a function of the dissipation parameter at a fixed value of the field amplitude. As the external field is increased, this resonant peak keeps shifting continuously in the direction of stronger dissipation.

IV. THEORETICAL ANALYSIS

In the semiclassical limit the effects of the radiation field are equivalent to those of a time-dependent driving term. The

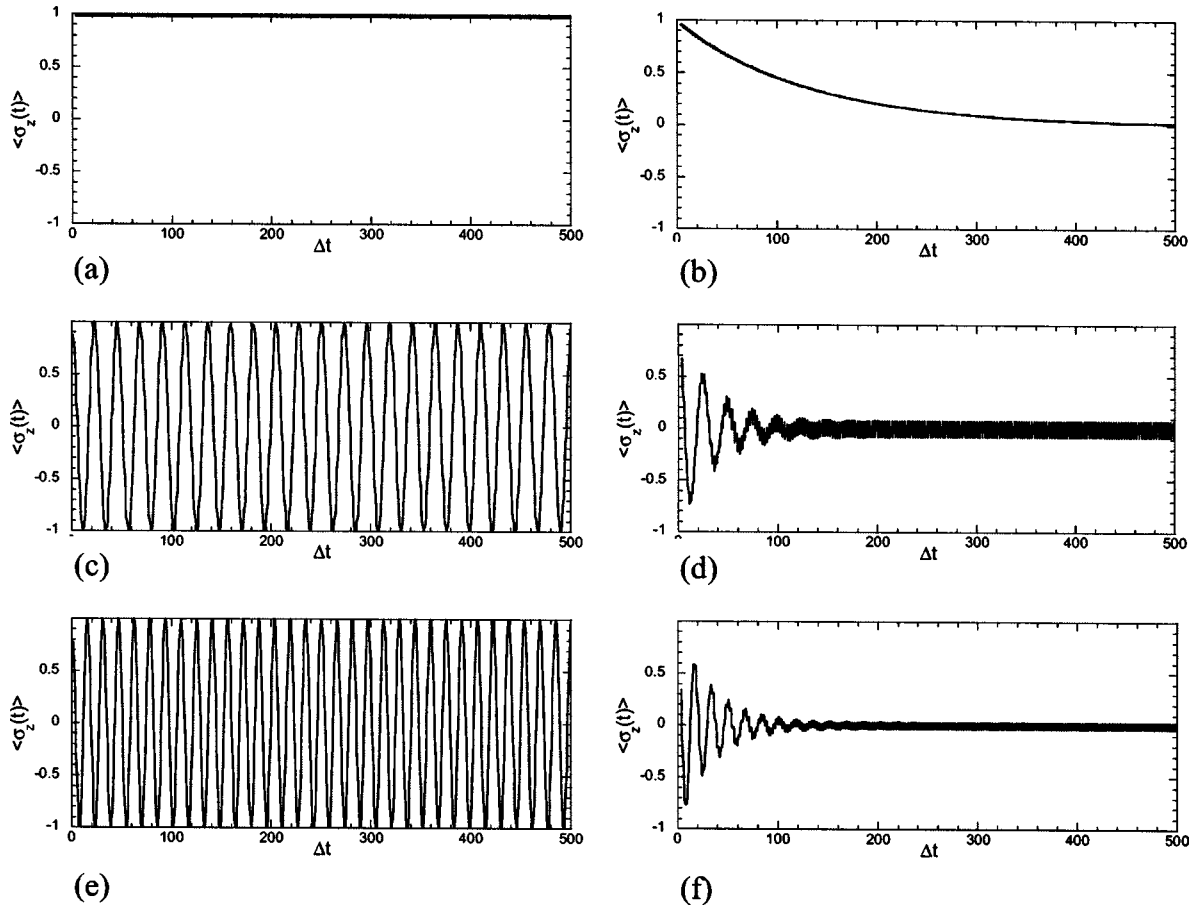


FIG. 1. The average position of the system as a function of time for $\omega=5\Delta$. (a),(b) $2V_0/\hbar\omega=2.3932$, corresponding to the first near-localization of the TLS observed in Fig. 2. At this point $J_0(2V_0/\hbar\omega)\approx 0$ (but note that J_0 vanishes at $2V_0/\hbar\omega=2.4048$). (c),(d) $2V_0/\hbar\omega=3.04$, corresponding roughly to the second maximum of the steady-state TLS amplitude. (e),(f) $2V_0/\hbar\omega=3.76$, corresponding to the first shallow minimum of the steady-state amplitude. At this point $J_1(2V_0/\hbar\omega)\approx 0$.

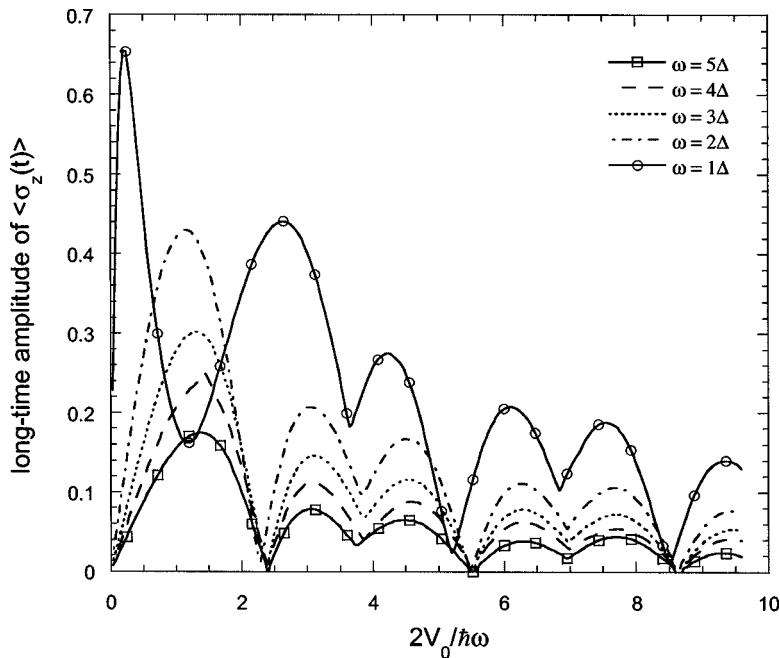


FIG. 2. The amplitude of coherent oscillation as a function of $2V_0/\hbar\omega$ for $\alpha=0.04$. The oscillation amplitude is recorded from the peak nearest to $t=80\times 2\pi/\Delta$, for five different driving frequencies, $\omega=\Delta, 2\Delta, 3\Delta, 4\Delta$, and 5Δ . The oscillation amplitudes show similar “interference patterns”. However, the system’s behavior at $\omega=\Delta$ is markedly different from all the others, and this is a clear manifestation of the breakdown of the perturbation theory, and its first peak corresponds to the quantum SR at the weak field and small dissipation limit.

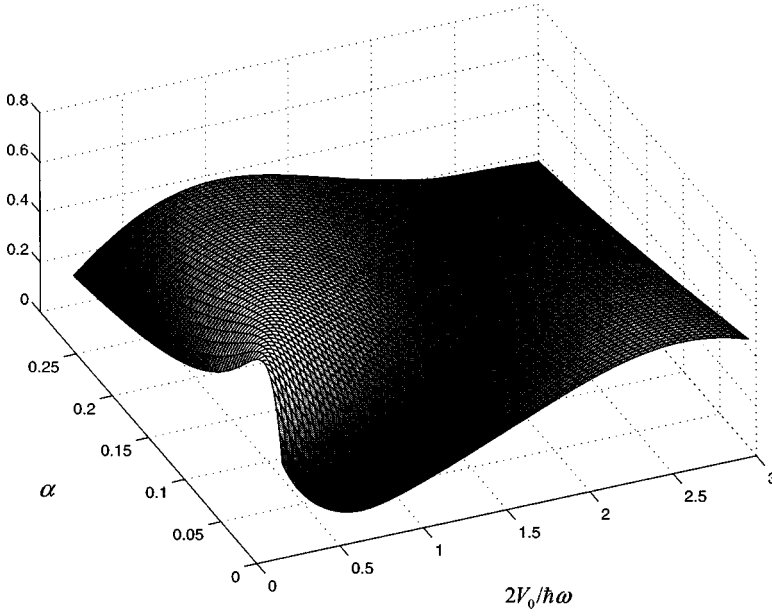


FIG. 3. The amplitude of the TLS coherent oscillation as a function of $2V_0/\hbar\omega$ and α . The position of the resonant peak continuously shifts toward the direction of stronger dissipation as the external field is increased.

latter is more convenient for carrying out numerical simulations of the ensuing dynamics. However, a theoretical analysis of the observed behaviors is facilitated by going back to the quantized representation of the radiation field. This way the Hamiltonian of Eq. (1) can then be rewritten in an equivalent form

$$\hat{H}_{\text{SFB}} = -\frac{1}{2}\hbar\Delta\hat{\sigma}_x + g\hat{\sigma}_z(\hat{a}^\dagger + \hat{a}) + \hbar\omega\hat{a}^\dagger\hat{a} + \frac{g^2}{\hbar\omega} + \sum_j \left[\frac{p_j^2}{2m_j} + \frac{1}{2}m_j\omega_j^2x_j^2 + c_jx_j\hat{\sigma}_z \right], \quad (6)$$

where \hat{a}^\dagger , \hat{a} are the boson creation and annihilation operators. For the time-dependent and quantized field representations to describe the same physical situation the coupling energy between TLS and field must satisfy the relation $g = V_0/\sqrt{2(2n+1)}$, where n is the quantum number that specifies the photon state. In the strong field limit $n \gg 1$ and $\sqrt{ng} \gg \hbar\Delta$ [23]. We consider high-frequency driving and choose $\omega \gg \Delta$.

A new set of dressed states $|\tilde{L}_n\rangle = \exp[-\xi(\hat{a}^\dagger - \hat{a})]|n\rangle \otimes |L\rangle$ and $|\tilde{R}_n\rangle = \exp[\xi(\hat{a}^\dagger - \hat{a})]|n\rangle \otimes |R\rangle$ can be introduced with $\xi = g/\hbar\omega$. It can be shown that $|\tilde{L}_n\rangle$ and $|\tilde{R}_n\rangle$ are the eigenstates of the field Hamiltonian $\hat{H}_F = g\hat{\sigma}_z(\hat{a}^\dagger + \hat{a}) + \hbar\omega\hat{a}^\dagger\hat{a} + g^2/\hbar\omega$ with the same eigenvalue $n\hbar\omega$. In this new representation the total system-field-bath Hamiltonian is given by [23]

$$\hat{H}_{\text{SFB}} = \sum_{m=0}^{\infty} \left(\hat{H}^{(m)} + \sum_{q=1}^{\infty} \hat{H}_{\text{cross}}^{(m,q)} \right) \quad (7)$$

with

$$\hat{H}^{(m)} = \left[m\hbar\omega + \sum_j \left(\frac{p_j^2}{2m_j} + \frac{1}{2}m_j\omega_j^2x_j^2 \right) \right] \hat{I}^{(m)} - \frac{1}{2}\hbar\Delta_m\hat{\sigma}_x^{(m)} + \sum_j c_jx_j\hat{\sigma}_z^{(m)}, \quad (8)$$

$$\hat{H}_{\text{cross}}^{(m,q)} = -\frac{1}{2}\hbar\Delta D_{m,m+q}(2\xi) [|\tilde{L}_m\rangle\langle\tilde{R}_{m+q}| + (-1)^q |\tilde{R}_m\rangle\langle\tilde{L}_{m+q}|], \quad (9)$$

$$\hat{I}^{(m)} = |\tilde{L}_m\rangle\langle\tilde{L}_m| + |\tilde{R}_m\rangle\langle\tilde{R}_m|, \quad \hat{\sigma}_x^{(m)} = |\tilde{L}_m\rangle\langle\tilde{R}_m| + |\tilde{R}_m\rangle\langle\tilde{L}_m|,$$

$$\hat{\sigma}_z^{(m)} = |\tilde{L}_m\rangle\langle\tilde{L}_m| - |\tilde{R}_m\rangle\langle\tilde{R}_m|, \quad \hat{\sigma}_z = \sum_{m=0}^{\infty} \hat{\sigma}_z^{(m)},$$

$$\Delta_m = \Delta D_{mm}(2\xi), \quad D_{kn}(\xi) = \langle k|e^{\xi(\hat{a}^\dagger - \hat{a})}|n\rangle. \quad (10)$$

The first part of \hat{H}_{SFB} describes an infinite series of independent tunneling doublets with intradoublet spacing $\hbar\Delta_m$ and interdoublet separation $\hbar\omega$. Because it contains no interdoublet coupling terms, the first term is responsible only for the low frequency dynamics of the physical system. On the other hand, each term in the second part $\hat{H}_{\text{cross}}^{(m,q)}$ describes a q -photon process associated with the m th subspace.

First we focus on the effects of the “zeroth order” term in Eq. (7),

$$\hat{H}_{\text{SFB}}^{(0)} = \sum_{m=0}^{\infty} \hat{H}^{(m)}. \quad (11)$$

In this zeroth-order description the Hamiltonian is represented by an infinite set of independent doublets with renormalized splittings $\hbar\Delta_m$, coupled to replicas of the same harmonic bath (since $[\hat{H}^{(m)}, \hat{H}^{(m')}] = 0$ for all m and m'). Suppose that the bath is initially in a state of thermal equilibrium with respect to its own Hamiltonian, such that the initial density matrix of the whole system factorizes

$$\hat{\rho}(0) = |\psi_{\text{SF}}(0)\rangle\langle\psi_{\text{SF}}(0)| \exp(-\beta\hat{H}_B)/Z,$$

where

$$\hat{H}_B = \sum_{m=0}^{\infty} \sum_j [p_j^2/2m_j + m_j\omega_j^2 x_j^2/2] \hat{I}^{(m)} = \sum_{m=0}^{\infty} \hat{H}_B^{(m)}$$

and

$$|\psi_{\text{SF}}(0)\rangle = |n\rangle \otimes |L\rangle = \sum_{m=0}^{\infty} D_{nm}(\xi) |\tilde{L}_m\rangle.$$

As a result, the driven TLS is equivalent to an infinite series of independent doublets with the m th doublet having an initial population $|D_{nm}(\xi)|^2$ on the left site, and the average position of the TLS at time t can then be shown to be

$$\begin{aligned} \langle \hat{\sigma}_z(t) \rangle &= \sum_{m=0}^{\infty} \langle \hat{\sigma}_z^{(m)}(t) \rangle = \sum_{m=0}^{\infty} Z^{-1} \text{Tr}_B [\langle \psi_{\text{SF}}(0) | \exp(-\beta \hat{H}_{\text{SFB}}^{(0)}) \\ &\quad \times \exp(i\hat{H}_{\text{SFB}}^{(0)} t/\hbar) \hat{\sigma}_z^{(m)} \exp(-i\hat{H}_{\text{SFB}}^{(0)} t/\hbar) | \psi_{\text{SF}}(0) \rangle] \\ &= \sum_{m=0}^{\infty} Z_m^{-1} \text{Tr}_B [\langle \psi_{\text{SF}}(0) | \exp(-\beta \hat{H}_B^{(m)}) \\ &\quad \times \exp(i\hat{H}^{(m)} t/\hbar) \hat{\sigma}_z^{(m)} \exp(-i\hat{H}^{(m)} t/\hbar) | \psi_{\text{SF}}(0) \rangle] \\ &= \sum_{m=0}^{\infty} D_{nm}(-\xi) D_{nm}(\xi) Z_m^{-1} \text{Tr}_B [\langle \tilde{L}_m | \exp(-\beta \hat{H}_B^{(m)}) \\ &\quad \times \exp(i\hat{H}^{(m)} t/\hbar) \hat{\sigma}_z^{(m)} \exp(-i\hat{H}^{(m)} t/\hbar) | \tilde{L}_m \rangle] \\ &= \sum_{m=0}^{\infty} D_{nm}(-\xi) D_{nm}(\xi) \langle \hat{\sigma}_z^{(m)}(t) \rangle_m \xrightarrow{n \rightarrow \infty, m \rightarrow \infty} \lim \langle \hat{\sigma}_z^{(m)}(t) \rangle_m, \end{aligned} \quad (12)$$

where $\langle \hat{\sigma}_z^{(m)} \rangle_m$ is the average position of the m th independent doublet with the initial condition

$$\hat{\rho}_m(0) = Z_m^{-1} \exp(-\beta \hat{H}^{(m)}) |\tilde{L}_m\rangle \langle \tilde{L}_m|.$$

The behavior of a system with the Hamiltonian $\hat{H}^{(m)}$ has been studied extensively and thoroughly [2]. This result agrees very well with the well-documented belief that a driven TLS (with $\omega \gg \Delta$) is equivalent [1] to a free TLS with renormalized tunneling splitting

$$\Delta_{\text{eff}} = \lim_{m \rightarrow \infty} |\Delta_m| = \Delta |J_0(2V_0/\hbar\omega)|,$$

where J_0 is the zeroth-order Bessel function of the first kind. Based on the well-understood behaviors of the dissipative TLS with an Ohmic bath, the behavior of the driven system in this regime should depend on the relation between αT and $\Delta_{\text{eff}}(\Delta_{\text{eff}}/\omega_c)^{\alpha/(1-\alpha)}$. Thus, at a series of points where

$$J_0(2V_0/\hbar\omega) = 0 \quad (13)$$

the intradoublet oscillation channel is cut off. In this zeroth order picture the driven TLS should remain perfectly localized in the absence of dissipation.

When the driven TLS is coupled to a dissipative bath, transitions can occur via the interdoublet coupling terms that constitute the second part of Eq. (7) and which generally are weaker. Thus, the steady-state amplitude of the driven dissi-

pative TLS is expected to be minimized when the localization condition (13) is satisfied. Indeed, Eq. (13) is satisfied for values of the field amplitude that correspond to the deep minima in Fig. 2, at which the TLS steady state amplitude nearly vanishes. Because tunneling takes place via interdoublet processes in this case, it is associated with high-frequency components of the dynamics.

Among interdoublet crossing terms, the dominant contribution comes from one-photon processes governed by the Hamiltonian

$$\sum_{m=0}^{\infty} \hat{H}_{\text{cross}}^{(m,\pm 1)}.$$

It can be shown that $\lim_{m \rightarrow \infty} D_{m,m\pm 1}(2\xi) = J_1(2V_0/\hbar\omega)$, where J_1 is the first-order Bessel function. Thus the Hamiltonian responsible for one-photon processes becomes

$$-\frac{1}{2} \hbar \Delta J_1(2V_0/\hbar\omega) \sum_{m=0}^{\infty} [|\tilde{L}_m\rangle \langle \tilde{R}_{m\pm 1}| - |\tilde{R}_m\rangle \langle \tilde{L}_{m\pm 1}|]. \quad (14)$$

This describes transitions between the left state of the m th doublet and the right state of doublets $m \pm 1$, thus providing the dominant interdoublet tunneling mechanism alluded to in the previous paragraph. Equation (14) describes a ladder process that occurs simultaneously over an infinite number of TLS doublets, as shown in Fig. 4, giving rise to the observed nonvanishing long time amplitudes characteristic of QSR. It is clear that when

$$J_1(2V_0/\hbar\omega) = 0 \quad (15)$$

the main channel connecting adjacent doublets is severed, and the long-time steady-state oscillation of $\langle \hat{\sigma}_z(t) \rangle$ is expected to have a minimum. This analysis explains the existence of secondary minima observed in Fig. 2, where the TLS amplitude becomes small without vanishing. Higher-order multiphoton terms, which are weaker than those described by Eq. (14), continue to “pump” the ladder process under this condition, resulting in nonzero (but small) QSR amplitudes.

Equations (13) and (15) indicate that there are at least two factors controlling the long-time behavior of $\langle \hat{\sigma}_z(t) \rangle$. The diagonal term $\hbar \Delta J_0(2V_0/\hbar\omega)$ determines how fast and to what extent the dissipative TLS tunnels back and forth between

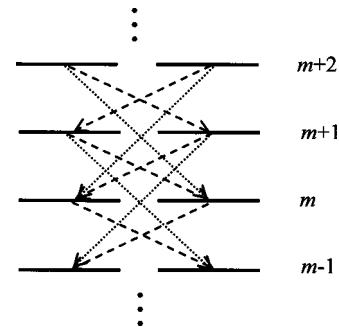


FIG. 4. Schematic representation of the tunneling doublets in the quantized representation of the radiation field.

the left and right sites of each doublet, while $\hbar\Delta J_1(2V_0/\hbar\omega)$ determines how efficiently these sites are repopulated via the interdoubt crossing processes. Competition between these mechanisms gives rise to the nonmonotonic variation of the steady-state amplitude observed in Figs. 2 and 3.

The analysis presented above applies only qualitatively to resonant (or near-resonant) driving. When the high-frequency approximation is not satisfied the TLS doublets are no longer sufficiently separated, and the hierarchy of crossing mechanisms breaks down, leading to considerable deviations from the described behaviors. For this reason the long-time TLS amplitude of the $\omega=\Delta$ curve shown in Fig. 2 displays a deep minimum, rather than a near-localization point, at a value of $2V_0/\hbar\omega$ that is smaller than the value corresponding to the first zero of J_0 .

V. CONCLUDING REMARKS

By performing accurate path integral calculations we have identified persistent high-frequency oscillations of a driven symmetric TLS coupled to dissipative environments in the strong-field, weak dissipation, and low-temperature regime. The oscillation amplitude exhibits complex patterns as the

parameters of the driving field are varied. Since the original discovery of the QSR phenomenon, much discussion has appeared, which has focused on the peak and subsequent decay of the TLS steady-state amplitude at a specific value of field strength. The present work shows that the oscillation amplitude does not decay indefinitely with increasing field, but rather exhibits subsequent peaks as well as deep and shallow valleys. These results constitute the extension of the QSR phenomenon discussed in earlier work to a much larger portion of parameter space.

We have also presented a theoretical analysis based on the quantized time-independent representation of the radiation field. This analysis allowed interpretation of the patterns observed in the numerical results. As shown in a recent paper [24], the complex patterns associated with QSR over a wide range of driving field strength and friction can be exploited to enhance and optimize the THz radiation emitted from double quantum well structures.

ACKNOWLEDGMENT

This work was supported by the National Science Foundation under Award No. CHE-0212640.

-
- [1] M. Grifoni and P. Hanggi, *Phys. Rep.* **304**, 229 (1998).
 - [2] A. J. Leggett *et al.*, *Rev. Mod. Phys.* **59**, 1 (1987).
 - [3] Y. Dakhnovskii, *Phys. Rev. B* **49**, 4649 (1994).
 - [4] D. E. Makarov and N. Makri, *Phys. Rev. E* **52**, 5863 (1995).
 - [5] N. Makri and L. Wei, *Phys. Rev. E* **55**, 2475 (1997).
 - [6] N. Makri, *J. Chem. Phys.* **106**, 2286 (1997).
 - [7] P. Jung, *Phys. Rep.* **234**, 175 (1993).
 - [8] D. E. Makarov and N. Makri, *Phys. Rev. B* **52**, R2257 (1995).
 - [9] M. Grifoni *et al.*, *Phys. Rev. E* **52**, 3596 (1995).
 - [10] M. C. Goorden and F. K. Wilhelm, *Phys. Rev. B* **68**, 012508 (2003).
 - [11] D. E. Makarov and N. Makri, *Chem. Phys. Lett.* **221**, 482 (1994).
 - [12] N. Makri and D. E. Makarov, *J. Chem. Phys.* **102**, 4600 (1995).
 - [13] N. Makri and D. E. Makarov, *J. Chem. Phys.* **102**, 4611 (1995).
 - [14] N. Makri, *J. Math. Phys.* **36**, 2430 (1995).
 - [15] E. Sim and N. Makri, *Comput. Phys. Commun.* **99**, 335 (1997).
 - [16] E. Sim and N. Makri, *Chem. Phys. Lett.* **249**, 224 (1996).
 - [17] N. Makri, *J. Phys. Chem.* **102**, 4414 (1998).
 - [18] R. P. Feynman and J. F. L. Vernon, *Ann. Phys. (N.Y.)* **24**, 118 (1963).
 - [19] G. Taft and N. Makri, *J. Phys. B* **31**, 209 (1998).
 - [20] K. Forsythe and N. Makri, *Phys. Rev. B* **60**, 972 (1999).
 - [21] M. Topaler and N. Makri, *J. Chem. Phys.* **101**, 7500 (1994).
 - [22] U. Weiss, *Quantum Dissipative Systems* (World Scientific, Singapore, 1993).
 - [23] P. Neu and R. J. Silbey, *Phys. Rev. A* **54**, 5323 (1996).
 - [24] K. Dong and N. Makri, *Chem. Phys.* **296**, 273 (2004).